RESEARCH STUDY OF THE PHOTOVOLTAIC EFFECT IN CADMIUM SULPHIDE

Jet Propulsion Laboratory
Contract No. 952666

SEMIANNUAL REPORT NO. 1
April 15, 1970

by

K. W. Böer
Principal Investigator
Physics Department
University of Delaware
Newark, Delaware 19711

RESEARCH STUDY OF THE PHOTOVOLTAIC EFFECT IN CADMIUM SULPHIDE

Jet Propulsion Laboratory
Contract No. 952666

SEMIANNUAL REPORT NO. 1
April 15, 1970

by

K. W. Böer
Principal Investigator
Physics Department
University of Delaware
Newark, Delaware 19711

This work was performed for the Jet Propulsion Laboratory, California Institute of Technology, as sponsored by the National Aeronautics and Space Administration under Contract NAS7-100.

ABSTRACT

Results of the first phase (0.5 year) of a three-year effort to improve the quality of CdS photovoltaic cells are presented. The primary research effort has been concentrated in three fields: (a) Theory related to the photovoltaic effect, (b) materials production and investigation of photovoltaic parameters, and (c) analysis of changes in photoelectric parameters caused by radiation damage and ambient atmosphere, crucial for reliable operation of photovoltaic cells. From results in section (a) information on doping and on grading of the heterojunction are obtained. In section (b) successful growth and doping of CdS platelets and production of Cu_xS heterojunctions are reported. In section (c) it has been shown that oxygen ambient changes photoelectric properties only in a thin ($\sim 10^{-5}$ cm) surface-near region and that this influence can be minimized by proper doping[1,2]. It is suggested that the threshold for X-ray damage depends on ambient and on the gradient of intrinsic defects near the surface. Preparations for the crucial set of experiments are completed.

SUMMARY

This report describes the results obtained in the first phase (0.5 year) of a six-phase program to improve the properties of a II-VI (currently CdS)-photovoltaic cell, specifically, to maximize the conversion efficiency.

The objectives during this first phase were to set-up a nine-man research team in this field, to familiarize each member with the state of the art and the general goal, and to concentrate with the three three-men groups of this team on the following subjects:

a. Theory of the photovoltaic effect with the final goal to determine maximum conversion efficiency for certain junction-devices and to identify important device parameters for the purpose of optimization.

b. Production and doping of the photoconducting material and its junction (CdS-platelets/Cu_xS -- later II-VI layers with optimized junction material), and to measure characteristic photoelectric properties.

c. Analysis of changes in photoelectric parameters critical for reliable operation of photovoltaic cells, caused by radiation damage and the ambient atmosphere.

This approach was taken since it seems to be the most economical one for achieving technically useful results, taking into consideration the previous experience of the members of the research team (six students, two post-doctoral fellows and the principal investigator) and already known results. As more proficiency is achieved by each team member and essential basic results become available, more technical goals related to the actual device will be attacked by members of the team.

At the end of the first phase it can be concluded that two groups of the team have increased our knowledge in the field, -- in the theory by

pointing out critical parameters of the device and practical steps for improvement, and experimentally by pointing out the reasons for the different sensitivity of CdS with different defect structure to ambient oxygen. The third group was successful in preparing CdS platelets with Cu_xS junctions properly doped for the suggested investigations and in performing the first set of photoelectric measurements.

On the basis of these results the following recommendations are made:

1. The thickness of the device should be smaller than the random-walk length of majority carriers in each region for maximized efficiency.

2. The center range of the band gap should have minimized defect-level density for maximized open-circuit voltage.

3. The junction should be graded with a gradient thickness not exceeding the Schubweg of minority carriers in the junction field.

4. The illumination should enter through the wide band gap material.

5. In backwall configuration an n^+-CdS layer with Ti/Al grid, desensitized to oxygen ad/desorption by a steep Cd-gradient should be used as the electrode.

The most significant features of the first phase of the work are (1) the familiarization of the team with the subject, (2) the theoretical recommendation obtained for certain important parameters and constructural elements of the photovoltaic device, and (3) experimental evidence for certain environmental influences critical for device stability, yielding recommendations on a Cd-surplus gradient near the surface, to minimize this influence.

TABLE OF CONTENTS

1. INTRODUCTION

Presently the basic understanding of the photovoltaic effect at an actual heterojunction is in its infancy. Though useful devices have been developed, many questions about the processes involved remain unanswered and the overall quality of these devices can at best be classified as fair with respect to desirable parameters, most prominently the conversion efficiency.

After the technology of producing photovoltaic cells has evolved to a degree where several types can be reproducibly manufactured it is paramount that we learn to analyse the complex formation procedure to be able to optimize the characteristics of these cells.

The necessary research in this respect can be subdivided into three fields:

a. Analysis of the physics of the photovoltaic effect with the goal

   1. to determine maximum conversion efficiencies for homo- and heterojunction cells for the solar spectrum and
   2. to identify clearly the important parameters of a photovoltaic cell for purposes of optimization.

b. Development of experimental methods to measure the important parameters (a.2), and

c. Selection of the most promising junction material and optimization of doping and grading of the junction.

In order to approach this goal on a wide front, simultaneous research projects in several of the above-mentioned fields were started in September 1969, some of them by redirecting earlier work in similar fields for strategic team work.

Most central is the complex on the theory of the photovoltaic effect, currently investigated by P. Massicot, G. Dussel and the Principal Investigator. Immediate interest is focussed on the active volume (junction plus adjacent minority carrier random walk regions), the spectral distribution of the optical absorption in this volume, and the electrical parameters of the junction. Pertinent information is obtained from a more detailed analysis of "blocking" contacts where experimental results are immediately available.

The second part of the research team (L. v. d. Berg, J. Phillips and H. Hadley) is concerned with preparing and doping the CdS crystals and producing the heterojunction (at this time Cu_2S/CdS) and investigating the electrical parameters of this system (current-voltage characteristics, high-field domains, spectral distribution of photoemf).

The third group (C. Wright, J. Bragagnolo and G. Storti) investigates properties of the CdS which are crucial for reliable operation under actual working condition, such as, e.g., radiation damage and influence of the ambient atmosphere.

As the work progresses and every member of the research team becomes sufficiently familiarized with the general field, more specific problems will be investigated, such as minority carrier lifetimes, the field distribution in the junction, controlled gradation (doping), epitaxial growth and optimization of recrystallization techniques.

2. TECHNICAL DISCUSSION

(a). The theoretical work on photocells is aimed at elucidating the relationships between the performance characteristics (e.g., open-circuit voltage, power, efficiency, resistance to radiation) and the quantities subject to technological control (e.g., doping, composition). At the present time, an

analytic solution to the equations that determine carrier behavior cannot be obtained because the equations are nonlinear. The usual approach has been to make approximations until the equations can be solved. We have adopted an alternative approach. We construct graphs of the relevant physical quantities as functions of the distance from an arbitrary plane normal to the current flow; namely, electron and hole concentrations (n and p), conduction and valence bands (E_c and E_v), electron and hole quasi-Fermi levels (E_{f_n} and E_{f_p}), electric field (F), space-charge density (ρ), electron and hole diffusion currents ($j_{n_{diff}}$ and $j_{p_{diff}}$), electron and hole drift currents ($j_{n_{dr}}$ and $j_{p_{dr}}$), and ionized donor and acceptor concentrations (N_D^+ and N_A^-). Graphs have been constructed for homojunctions. (When heterojunctions are considered one must take into account other types of currents, besides those due to drift and diffusion, which arise because of variations in the band gap.) These curves are constructed in the following manner:

a. Reasonable assumptions are made as to the behavior of n(x), p(x), $N_D^+(x)$, and $N_A^-(x)$. For example, we assume that the carrier densities are constant outside of the junction and that n(x) and p(x) decrease rapidly as we enter the junction from the n-type and p-type regions respectively. We also assume that the ionized-impurity concentrations are constant outside of the junction and decrease gradually in the junction. These curves are iterated in a self-consistent fashion with the other curves. From these quantities $\rho(x)$ is determined.

b. Working backwards from $\rho(x)$ we draw the curves of F(x) and V(x), where V(x) is the potential, using the relations

$$\frac{dF}{dx} = -\frac{e}{\epsilon\epsilon_o}\rho \qquad (1)$$

$$\frac{dV}{dx} = -F \quad , \qquad (2)$$

where e is the electronic charge, ϵ_o is the permittivity of free space, and ϵ is the dielectric constant. $E_c(x)$ and $E_v(x)$ can be determined from V(x). (In the case of a heterojunction, the behavior of the electron affinity $\chi(x)$ must be known.)

c. E_{f_n} and E_{f_p} are inferred from the equations

$$n = N_c \exp -\left[\frac{E_c - E_{f_n}}{kT}\right] \qquad (3)$$

$$p = N_v \exp -\left[\frac{E_{f_p} - E_v}{kT}\right] \qquad (4)$$

$$j = j_n + j_p = -ne\mu_n \frac{dE_{f_n}}{dx} - pe\mu_p \frac{dE_{f_p}}{dx} \qquad (5)$$

and knowledge about j (j is constant as a function of x; j = o under open-circuit conditions.) In these equations N_c and N_v are the effective densities of states in the conduction and valence bands, k is Boltzman's constant, T is the temperature, and $\mu_{n,p}$ are the mobilities of the carriers (assumed constant).

d. The graphs of the various currents are obtained by utilizing their defining relations in terms of previously graphed quantities:

$$j_{n_{dr}} = ne\mu F \qquad (6)$$

$$j_{n_{diff}} = \frac{\mu_n kT}{e}\frac{dn}{dx} \qquad (7)$$

and similarly for the hole currents.

Two types of information are obtained from these curves: (1) qualitative information, and (2) information which enables us to construct approximate solutions if necessary. Qualitative information includes, for example, the location of critical points of the curves, such as those where $\frac{dV(x)}{dx} = -F = 0$. At the points where F = 0 the drift current is zero and all current is carried by diffusion.

We have obtained two very useful results from the graphs for a p-n junction photocell: In order to maximize the open-circuit voltage one must (a) have the Fermi-level as close to the respective bands as possible before illumination (This is preferably done by slight doping.); and (b) upon illumination shift the quasi-Fermi levels for minority carriers as close as possible to their bands, i.e., make the material as nearly ambipolar as possible (This is also done by doping.). Condition (b) has been confirmed experimentally via measurements of minority carrier lifetimes[3].

Another parameter which one can vary is the junction width. We have considered this problem with respect to both homojunctions and heterojunctions. In the case of a homojunction, the optimum width depends on several considerations, which will be discussed below. First of all, we should introduce the parameters necessary to describe the microscopic processes taking place during power generation. These parameters are the random-walk lengths for recombination, $\Lambda_{n,p}^{(n)}$ and $\Lambda_{n,p}^{(p)}$ (The superscript denotes whether Λ refers to the n- or p-type region; the subscript identifies the carrier referred to.), the intrinsic optical absorption length $d(\lambda) = \kappa(\lambda)^{-1}$ ($\kappa(\lambda)$ is the optical absorption coefficient), the Debye length L_D, and the Schubwegs $\Delta_{n,p}$ ($\Delta_{n,p}$ are the random-walk lengths for recombination if the carriers are drifting in an electric field.). The junction width ℓ is defined as the width of the region in which there is a built-in electric field. To optimize photocell performance,

we should realize several conditions:

1. The region which is active for optical absorption is $\Lambda_n^{(p)} + \ell + \Lambda_p^{(n)}$. Thus we want

$$\Lambda_n^{(p)} + \ell + \Lambda_p^{(n)} \geq d(\lambda) \tag{8}$$

If this condition does not hold, electron-hole pairs will be excited optically outside of the region where they can contribute to power generation.

2. We would like to have the junction as narrow as possible, consistent with Eq. (8), so that the electric field in the junction, and hence the drift current, is maximized. At least we should have

$$\ell < d(\lambda) \tag{9}$$

3. A minority carrier that reaches the junction should be swept through the junction before it is killed. This implies

$$\Delta_{n,p} > \ell \tag{10}$$

4. In the case of a homojunction, L_D is essentially a measure of ℓ, so there is no additional condition to be imposed with respect to L_D.

5. Obviously an auxiliary condition is to maximize $\Lambda_n^{(p)}$ and $\Lambda_p^{(n)}$. This will maximize the number of minority carriers that can migrate to the junction and contribute to power generation. One of the goals for the immediate future is to determine the optimum width quantitatively.

Before making any detailed remarks about investigations into Cu_2S:CdS heterojunction behavior, we would like to make some general comments about the state of the art. Advances in the theory are hampered by lack of firm experimental knowledge of fundamental quantities. For example, there is even uncertainty as to the band-gap energy of Cu_2S. Some authors[4,5] have inferred

a value of approximately 1.2 eV; another has inferred one of 1.0 eV[6]. Others[7,8] have obtained a value of about 1.8 eV. An examination of the experimental conditions described in each of the papers leads one to the conclusion that the value of 1.8 eV is on firmest ground, but one cannot yet be sure. Moreover, the electron affinity of Cu_2S is not known, although an indirect estimate is available[4]. To cloud the picture further, $Cu_{2-x}S$ can exist in several phases besides that with $x = 0$, and one must be careful in drawing conclusions from publications in which the phase of $Cu_{2-x}S$ has not been conclusively identified. In view of these questions, while the experimental knowledge about Cu_2S:CdS heterojunctions is being solidified we have adopted the strategy of attempting to determine theoretically the characteristics of the best possible heterojunction. Then we will endeavor to find the optimum materials and technology to enable us to fabricate practically a heterojunction photovoltaic cell whose performance approaches as closely as possible the performance of the ideal.

In line with this strategy we have considered the question of abrupt vs. graded junctions. The existence of a "notch" or "spike" in the conduction or valence band of an abrupt heterojunction appears to have a deleterious effect on the photovoltaic performance of the junction[9]. Therefore we have examined the possibility of grading a junction, and we tentatively conclude that by doing this one can eliminate the harmful effects of the discontinuities at an abrupt junction.

We can make an analysis of the optimum width of the heterojunction which is similar to the previous analysis for a homojunction. However, there are two additional considerations in the case of a heterojunction. First of all, since the graded region does not have translational symmetry, it must be considered as a quasi-single-crystal with a position-dependent band gap[10,11],

and some of the parameters will depend on position due to this fact. Therefore, when these parameters are used in reference to heterojunctions, they are to be understood as representing "appropriately averaged" quantities. Quantitative development of this averaging process is being carried out. Secondly, there are two "widths" one can define. One is ℓ, which is the same as for a homojunction (and again closely related to the Debye length). The other is ℓ_G, which is the width of the graded region. There are two conditions on ℓ_G. One is that it be large enough so that the harmful effects of a notch and/or spike be eliminated. The other is that, consistent with the previous statement, $\ell_G \simeq \ell$. This is so that the electric field due to space charge (existing over the distance ℓ) and the effective electric field due to band-gap grading[12] (existing over the distance ℓ_G) are concentrated in the same region. With the above-mentioned modifications taken into account, we can apply the conditions previously established for homojunctions to heterojunctions. Further work on heterojunctions aimed at incorporating these conditions into a quantitative theory is presently being carried out.

One additional point to be considered is the collection of the carriers. To maximize efficiency we want to collect the maximum number of carriers by the electrodes before they are killed. E.g., after the photogenerated electrons have been swept into the n-region we want the distance they have to travel to the electrodes to be less than $\Lambda_n^{(n)}$. Thus we want the thicknesses of the n- and p-regions to be less than $\Lambda_n^{(n)}$ and $\Lambda_p^{(p)}$ respectively.

As discussed elsewhere in this report (Sec. 2.b), the high-field domain technique[13] is being used to study the heterojunction. Therefore, it is of importance to clarify the relation between the boundary of the domain (in this case the heterojunction) and the value of the field within the domain.

From this relation one expects to derive information about the heterojunction itself.

Due to the availability of proper crystals, experimental set-up and data, it was easier to initiate this study with the test case of a blocking contact to a CdS crystal[14,15]. This case has the advantage, besides the simplicity introduced by the fact of dealing with a homogeneous material, of having interesting technological applications, e.g., a better understanding of the gain factor and response time of a photoconductor with a blocking contact.

The experimental study is being conducted by Dr. R. Stirn at Jet Propulsion Laboratory. In this discussion, the preliminary theoretical results will be presented, and an attempt to interpret in general the experimental results will be made.

Two kinds of experiments have been conducted: (1) The determination of the value of the field within the domain and saturation currents as a function of light intensity, temperature, metal contacts, and doping (these latter by H. Hadley of our Laboratories), and (2) The measurement of the transient of the current when the voltage is applied suddenly and how the stationary state is obtained.

(1) Experimental results[14,15] confront us with the following situation: (a) the current is too large for a blocking contact (i.e. the gain factor is larger than one and the current is much larger than the "thermoionic" current at these temperatures using known values of the work function obtained at zero current). (b) The fields within the domains (at distances comparable to the mean free path of majority carriers from the cathode) are too small to allow tunneling directly. Therefore either tunneling does not take place or there is a high density of positive charge immediately adjacent to the cathode to build up the necessary tunneling field.

An attempt was made to explain the experimental results by a reduction in the barrier caused by a positive space-charge layer very close to the cathode. With a more detailed analysis we find that we cannot explain the results in this way. Free holes cannot be "pinned" down close to the cathode; the image force from the metal is attractive and too strong at short distances to be overcome by any other force. To generate the required reduction of the barrier a total of 10^{13} holes is required. However, from the fact that the gain factor for hole currents is much smaller than one, only an amount equal to $a \cdot \Lambda_p$ can reach the cathode per cm^2 and second (where a is the number of pairs generated per $cm^{-3}s^{-1}$, and the random-walk distance $\Lambda_p \lesssim 10^{-5}$ cm). Therefore, even with total collection efficiency (i.e., all holes generated within a distance Λ_p contribute to the space-charge region, that is, they do not recombine), with the experimental value of $a \simeq 10^{14} cm^{-3}s^{-1}$, it would take 10^4s to form the space-charge layer. This time is too long compared with experimental values.

The large space charge could be due to a high density of trapped holes. A high density of hole traps is not observed experimentally in these crystals. If hole traps with the known densities would accumulate charge, the space-charge layer would extend too far from the cathode and tunneling would be observed. In this case, from a detailed analysis of the restrictions imposed by the field of directions[14] it is concluded that saturation currents should correspond to the minimum value[13], a fact which is contrary to experimental observation. In addition, the same kinetic arguments relating to the provision of holes as in the case of free holes apply here. Moreover, if there were a high density of deep hole traps close to the cathode, then tunneling of electrons from the metal would keep the occupation of these traps low, thus reducing the space charge and the field.

From the previous discussion it is clear that the large currents observed experimentally are due to either:

a. a reduction of the work function by a change in its dipole part, at the proper boundary[16]; or

b. tunneling through the barrier.

We will discuss the possibility of tunneling in more detail, with the crucial consideration being the storage of a high density of positive charge next to the cathode. In this case it will also be necessary to explain why a saturation current larger than the minimum is observed (or equivalently, why the field within the domain is substantially lower than the known tunneling fields).

In the neighborhood of the cathode, an ionized donor produces locally a positive charge, that by bending the conduction band down in its neighborhood, may contribute substantially to easing the process of tunneling[17]. In this way tunneling fields are reduced from the usual value of 10^6 V/cm to a value of the order of 3×10^5 V/cm (This also depends on the density of centers, etc.).

Although this field is sufficient for tunneling, it is higher than the field in the domain. Therefore there must be a transition region (with a width on the order of the mean free path of the majority carrier), between the tunneling region and the domain, where a net positive charge is stored to reduce the field. Usually, hole traps are acceptors, and therefore, when the hole is captured, the center becomes electrically neutral. This leaves a neighboring ionized donor electrically uncompensated, and this has a net positive charge. Uncompensated donors close to the cathode can be produced by: (a) The mechanism discussed above; namely, by bringing in a hole to the neighboring compensating acceptor (not sufficient in the present case, see

the discussion related to free holes above).

(b) Extracting the electron from the neighboring compensating acceptor (e.g., by tunneling). This mechanism is not of importance here because it would not help reduce the tunneling field to the domain field. See the following discussion.

(c) Extracting the electron from a chemically uncompensated deep donor (i.e. from a donor below the initial position of the dark Fermi-level, such that it is initially not ionized), through either tunneling or field-enhanced ionization[18] (FEI). From kinetic experiments one cannot derive information about such a kind of center, nor about its density, since it would never act as an effective hole trap, except under the conditions discussed here.

The necessary density of these centers can be derived from Poisson's equation and the fact that the field decreases to the value within the domain (F_{II}) in a distance of the order of the mean free path of majority carriers (λ). Therefore

$$\frac{dF}{dx} \simeq \frac{\Delta F}{\lambda} \approx \frac{e}{\varepsilon\varepsilon_o} \rho_1 \tag{11}$$

For $\Delta F = 2.5 \times 10^5$ V/cm, $\lambda = 2 \times 10^{-6}$ cm, one obtains

$$\rho_1 = 1.5 \times 10^{18} \text{ cm}^{-3} = N_D - n_D = N_D^+ \tag{12}$$

N_D is the concentration of donors and n_D the concentration of electrons in donors. The occupancy of these levels is determined by kinetic equilibrium; i.e., the rate of capture equals the rate of emission, or

$$\frac{j_n}{e} q(F) \ (N_D - n_D) = \alpha(F) \ n_D \tag{13}$$

where $q(F)$ and $\alpha(F)$ are the field-dependent capture cross-section and emission probability, respectively.

$$\frac{n_D}{N_D} = \frac{\frac{j_n\, q(F)}{e\ \alpha(F)}}{1 + \frac{j_n\, q(F)}{e\ \alpha(F)}} \tag{14}$$

Therefore

$$\frac{dF}{dx} = -\ 10^{-7}\ N_D\ \left(1 - \frac{j_n\, q(F)}{e\ \alpha(F) + j_n\, q(F)}\right) \tag{15}$$

It is clear that when the charge is generated by the process of tunneling, the only quantity affected by the field is the emission probability $\alpha(F)$, which increases strongly for fields above threshold[19]. Therefore, below threshold $e\alpha(F) << j_n q$ and $\frac{dF}{dx} << -10^{-7} N_D$. This implies that the field cannot decrease rapidly below threshold, and F_{II} would be of the order of the tunneling fields.

If, however, the mechanism for generating space charge is FEI, which has a much smaller threshold, then at fields below those required for tunneling through the barrier there is still a substantial space charge, and the field will be decreased in a short distance, depending on the availability of ionizable donors. The threshold field (i.e., F_{II}), should be obtained from the condition

$$e\ \alpha(F_{II}) \simeq j_n\, q(F_{II}) \tag{16}$$

For the mechanism of FEI, using $j_n = 10^{-5}$ a/cm^2, and the field dependence of $\alpha(F)$ and $q(F)$ derived in reference 18, at T = 200° K and E_D = 0.7 eV (approximately the position of the dark Fermi-level), one obtains $F_{II} \simeq 10^5$ V/cm.

From the field dependence of $\alpha(F)$ and $q(F)$, one can also obtain an implicit expression for the dependence of F_{II} on the temperature, which can be written as

$$\sqrt{\frac{e\ F_{II}}{\varepsilon\varepsilon_o}} = E_D + kT\ \ln\ [f(F_{II}/T^2)], \tag{17}$$

where f(x) is a quotient of polynomials of x, and therefore a not-too-strong function of T. This would explain the experimental observation that F_{II} does not change substantially with temperature in the range between 150° K - 300° K, as one would expect from a rather intuitive model. A quantitative analysis of the temperature dependence has not yet been attempted.

In summary, it is found that tunneling through the barrier is a possible mechanism for provision of the current observed in CdS, provided that there is a sufficiently high density of deep donor levels, which would be inactive in photoconductivity processes. The field in the domain would be determined by Eq. (16). The fact that F_{II} is lower than the tunneling fields in the case of CdS indicates that some other mechanism, most probably FEI, is responsible for the generation of the space charge.

(2) The transient behavior of the current could be obtained by solving the Poisson, transport and kinetic equations simultaneously, with proper consideration of boundary conditions. Clearly, the system of equations is nonlinear, and a closed solution is unobtainable. In the following discussion we will attempt a very simplified model, which we expect will give the essentials of the time dependence of the current.

Previous to the application of the voltage, the crystal is assumed to be homogeneously illuminated, with one ohmic anode and a perfectly-blocking cathode (i.e., one that allows no transport of electrons from the metal electrode). It is assumed that there are no internal fields at $t \leq 0$, and therefore the quasi-Fermi level (QFL) for electrons, E_{f_n}, is flat and at the same depth from the conduction band everywhere in the crystal (the Schottky barrier at the cathode is neglected; some of the effects of the barrier are incorporated into the non-transparent contact assumed). There is a trap level

distribution of density N(E)dE at energy E below the conduction band. For $E > E_{f_n}$, the traps are totally occupied with electrons (n(E)dE = N(E)dE), while above the QFL they are increasingly empty ($n(E) = N(E) \exp [-(E-E_{f_n})/kT]$). After application of the voltage ($t \geq 0$), a field appears on the crystal (within the relaxation time of the metal electrodes). Free electrons are swept out by the field, and the traps begin to empty (outgassing). With increasing distance from the cathode (x = 0), the particle current increases (due to the perfectly blocking contact, at t = 0, $j_n (x = 0) = 0$). Within distances large compared to the mean free path, n thermalizes and can be obtained from $n(x) = j_n(x)/e\, v_{dr}$ (neglecting diffusion currents). The outgassing of traps builds up the particle current, since the trapped charge is much greater than the free charge, i.e.

$$j_n(x) = -e \int_0^x dx' \int_{E_v}^{E_c} \frac{\partial n(E)}{\partial t} dE = -e \int_0^x dx' \int_{E_v}^{E_c} [\alpha(E) n(E) - \beta\, n(x')(N(E) - n(E))]\, dE$$

or

$$j_n(x) = -e \int_0^x dx' \left(\int_{E_v}^{E_{f_n}} \beta\, N(E) e^{-\frac{E-E_{f_n}}{kT}} (n_o - n(x')\, dE + \int_{E_{f_n}}^{E_c} \beta\, N(E)\, (n_o - n(x')\, dE \right) \qquad (18)$$

where $\alpha(E) = \beta(E)\, N_c e^{-\frac{E}{kT}}$ and $n_o = N_c e^{-\frac{E_{f_n}}{kT}}$ have been used. The separation between shallow ($E < E_{f_n}$) and deep ($E > E_{f_n}$) traps has been made for simplicity in calculations. At the point Δx where $n(x) = n_o$ (the quasi-thermal equilibrium density of free carriers), there is no more outgassing. Since for $x < \Delta x$, $n(x) < n_o$, in a zero-order approximation one can write, neglecting n(x) compared to n_o,

$$j_n(x) = - e \int_o^x dx' \frac{\partial \rho_1(t)}{\partial t} \tag{19}$$

$$j_n(\Delta x,t) \simeq - e\Delta x \frac{\partial \rho_1(t)}{\partial t} \equiv e\Delta x\, f(t) \tag{20}$$

(The outgassing, which depends on the occupancy of the levels, is time-dependent.)

Since the traps are emptying, and initially the crystal was neutral, a space charge is built up near the cathode, i.e.

$$\begin{aligned} \rho_1(x,t) &= \int_{E_v}^{E_c} dE\, [n(E,t=0) - n(E,t)\,] = \int_{E_v}^{E_c} dE \int_o^t \frac{\partial n(E,t')}{\partial t} dt' \\ &= \int_o^t dt' \left(\int_{E_v}^{E_{f_n}} \beta\, N(E)\, e^{- \frac{E-E_{f_n}}{kT}} (n_o - n(x)\,)\, dE \right. \\ &\quad \left. + \int_{E_{f_n}}^{E_c} \beta\, N(E)\, (n_o - n(x)\,)\, dE \right) \end{aligned} \tag{21}$$

This space charge forces a redistribution of the electric field. Within the same approximation as before, one obtains

$$F(x,t) = F(o,t) - \frac{e}{\varepsilon\varepsilon_o} \int_o^x \rho_1(x',t)\, dx' \tag{22}$$

One can now integrate the field over the crystal length, and using the fact that the applied voltage is time independent, one obtains

$$V = \int_o^L F(x,t)\, dx = F(o,t)\, L - \frac{e}{\varepsilon\varepsilon_o} \int_o^L dx \int_o^x \rho_1(x',t)\, dx'$$

Using $\rho_1(x,t) = \rho_1(t)$ for $x < \Delta x$, and $\rho_1(x,t) = 0$ for $x > \Delta x$, we obtain

$$F(o,t) = \frac{V}{L} + \frac{e}{\varepsilon\varepsilon_o}\,\rho_1(t)\,\Delta x\,\left(1 - \frac{\Delta x}{2L}\right) \tag{23}$$

and

$$F(\Delta x,t) = \frac{V}{L} - \frac{e}{\varepsilon\varepsilon_o}\,\rho_1(t)\,\frac{\Delta^2 x}{2L} \tag{24}$$

In the region where there is no space charge (i.e., when $n(x) = n_o$, i.e. when $x > \Delta x$), the current is the current in the bulk $j(x,t) = j(\Delta x,t) = j_{bulk}(t)$, which is also essentially the measured current, since the field in the bulk is small and therefore the contribution of the displacement current is negligible there). Using $j_b(t) = e\mu n_o F(\Delta x,t)$, and Eq. (20), one obtains

$$\Delta x(t) = \frac{j_b(t)}{e\,f(t)} = \frac{\mu n_o\,F(\Delta x,t)}{f(t)} \tag{25}$$

and Eq. (24) becomes

$$F(\Delta x,t) = \frac{V}{L} - \frac{e}{\varepsilon\varepsilon_o}\,\frac{(\mu n_o)^2}{2L}\,\frac{\rho_1(t)}{f^2(t)}\,F^2(\Delta x,t)$$

or

$$F^2(\Delta x,t) + K(t)\,F(\Delta x,t) - K(t)\,\frac{V}{L} = 0 \tag{26}$$

where

$$K(t) = \frac{\varepsilon\varepsilon_o\,2L}{e(\mu n_o)^2}\,\frac{f^2(t)}{\rho_1(t)} \tag{27}$$

At $t = 0$, $K(0) = \infty$ (since $\rho_1(0) = 0$), and $F(\Delta x,0) = F(x,0) = V/L$. As t increases, f(t) decreases (there are less electrons to be outgassed) and $\rho_1(t)$ increases, and therefore K(t) decreases. For times such that $K(t) \ll V/L$, the solution of Eq. (26) becomes

$$F(\Delta x,t) \simeq \left[K(t)\,\frac{V}{L}\right]^{1/2} = \frac{f(t)}{\mu n_o}\sqrt{\frac{2\,\varepsilon\varepsilon_o}{e}\,\frac{V}{\rho_1(t)}} \tag{28}$$

and

$$j(t) = e\, f(t) \left[\frac{2\, \varepsilon\varepsilon_o\, V}{e\, \rho_1(t)} \right]^{1/2} \tag{29}$$

$$\Delta x(t) = \left[\frac{2\, \varepsilon\varepsilon_o\, V}{e\, \rho_1(t)} \right]^{1/2} \tag{30}$$

i.e., the space-charge region (Δx) contracts and the current decreases. At the same time, the field at the boundary increases, as obtained from Eq. (23)

$$F(o,t) \simeq \frac{V}{L} + \left[\frac{2\, e}{\varepsilon\varepsilon_o}\, \rho_1(t)\, V \right]^{1/2} \tag{31}$$

It may therefore reach values such that some other field-induced processes start at the cathode. One such process is FEI from deep non-ionized donors. Another is Zener extraction (tunneling out of deeply trapped electrons). The first process, depending on the energy of the donor, may require a smaller field, and therefore would occur first. From the discussion in the previous section, there should be a high density of deep levels in these crystals that could be activated by this mechanism. Due to the higher density, above a convenient "threshold" field, the outgassing from these levels can become much more important than the thermal outgassing from shallower levels. In order to deal with this situation, a simplifying assumption is that the escape rate is an on-off field-dependent rate (i.e., the mechanism is inactive below the threshold field, and is field-independent above this value). Calling F_c the threshold field and x_1 the point where $F(x_1,t) = F_c$ (the field increases monotonically from anode to cathode), and following the same procedure as before one obtains a relation between x_1 and Δx, namely

$$\frac{e}{\varepsilon\varepsilon_o} \frac{\rho_2\, x_1^2}{2L} = \frac{e}{\varepsilon\varepsilon_o} \rho_1 \Delta x \left(1 - \frac{\Delta x}{2L}\right) - \left(F_c - \frac{V}{L}\right) \tag{32}$$

where $\rho_2(t)$ is the charge density in the region $x < x_1$. It is obtained from

an equation similar to Eq. (21) if the field-dependence of the parameters is included.

Using this value of x_1 in the expression for the field, one obtains for the field in the bulk the expression

$$F\ (\Delta x,t) \ = \ F_c - \frac{e}{\varepsilon\varepsilon_o} \rho_1(t)\ \Delta x(t)\ [1 - \frac{\Delta x}{2L}\ ] \qquad (33)$$

This indicates that if $\rho_1\ \Delta x$ decreases, then the field in the bulk, and therefor the current, can increase. However, $\rho_1\ \Delta x$ won't be able to decrease until the current provided at x_1 becomes comparable to $j(t)$. In this case instead of Eq. (20) one uses

$$e\ \Delta x\ f(t) \ = \ j(t) - j_n(x_1,t) \qquad (34)$$

and replacing Δx in Eq. (33) one finds

$$F(\Delta x,t) \ \approx \ \frac{F_c + \frac{e}{\varepsilon\varepsilon_o} \rho_1(t)\ \frac{j_n(x_1,t)}{e\ f(t)}}{1 + \frac{e}{\varepsilon\varepsilon_o} \mu\ n_o\ \frac{\rho_1(t)}{f(t)}} \qquad (35)$$

When the second term in the numerator takes over, the field in the bulk, and therefore the current, starts to increase. $j_n(x_1,t)$ may increase in this regime because, in spite of the decrease of x_1, the field in $x < x_1$ is increasing towards the cathode, and the larger the field the faster the excitation rate. When the deep traps in the region $x < x_1$ start to be depleted the current should decrease. However, this cannot occur unless the field in the bulk decreases. Therefore, the "high" field region (limited by x_1), moves out from the cathode. This has two effects: (a) it keeps a "large" outgassing current (since part of this region was previously inactive), and (b) it increases the voltage drop in this region, thus allowing a decrease of the field in the bulk. Therefore, at this time the current decreases slowly.

Meanwhile, the field at the proper cathode (F(o,t)) keeps growing, until it reaches such a value that the perfectly blocking assumption is no longer valid, and replenishment occurs by tunneling through the barrier. This leads to the final equilibrium value of the current.

To summarize: The current will first jump to its "ohmic" value, (i.e., = $e\mu n_o \frac{V}{L}$), then decrease (thermal outgassing regime, Eq. (29)). While outgassing, the space charge close to the cathode increases. This increases the field in this region, until eventually it will reach a value such that some field-enhanced process is activated. This will provide a second outgassing mode in this region of the crystal. It can lead to an increase of the current in this second regime, until the activated deep traps are depleted. In order to maintain the current, this "high" field region grows out of the cathode, reducing the field in the bulk, and therefore the current. Finally the field at the cathode will reach tunneling values, replenishment of electrons will take place, and the current will grow to its final steady-state value. Thus it is concluded that the current first overshoots, then undershoots, and, if proper mechanisms are available, a second minimum can occur before the final equilibrium value is obtained.

The qualitative description of the behavior of the current as a function of time agrees with the experimental observations. Time constants for the decrease and increase of the current can be easily obtained for an assumed trap distribution in energy (that would fix the form of the functions f(t) and $\rho_{1,2}(t)$). Order-of-magnitude estimates have been made that agree reasonably well with the observed values.

For a different type of crystal, in which FEI may not be effective, the maximum after the first minimum should not appear, if tunneling out of

deep traps requires a higher field than tunneling through the barrier. However, the undershoot should be present, since an equation similar to (35) is valid under these conditions.

These results are preliminary, and they need further check of consistency of the results, validity of the approximations, and a careful analysis of its implications as applied to CdS and other materials.

(b). The activities in the crystal growth field during the last six months can be divided into two main areas:

1. Pure crystals have been grown to provide base material for the production of crystals with a Cu_2S-CdS junction and for secondary doping of CdS crystals with Cu to study conditons for the formation of inhomogeneities. Investigations of the conditions for growth required to obtain the desired effects in the crystal have been continued on the basis of previously obtained results. The influence of the composition of the carrier gas stream on the class of crystal obtained (Class I or II: Gross -Novikov classification[20] -- see Sec. 2.c.) has been established and is in agreement with the current interpretation on a microscopic scale of the difference between these two types. Class I crystals, with a higher relative concentration of cadmium in the surface-near region of the crystal, are obtained at low concentration (< 1.5 % vol.) of hydrogen sulfide in the carrier gas, while Class II crystals are obtained at higher concentrations. The effect of the temperature has not been clearly established yet, since its presumed influence is not so straightforward. The temperature-related influence can be threefold:

i. Actual temperature at which the crystal grows.

ii. Temperature to which the crystal is cooled down in the carrier gas atmosphere before it is removed from

the growth tube and exposed to air.

iii. Temperature gradient in the growth region.

2. Crystals of CdS doped with Cu have been grown by inserting a boat containing CuS in the carrier gas stream. This method was used to determine the effect of the dopant on the crystal growth properties. The growth conditions of a crystal in an atmosphere consisting of N_2, H_2S, CdS and CuS have been estimated using the same method as used for the pure crystals by assuming that the crystals grow under near-equilibrium conditions. The prevalent effect of a dopant which is incorporated in the crystal as an acceptor is that it reduces the vapor pressure of the crystal, and as such it decreases the partial pressure of the growing crystal compared with a pure crystal at the same temperature. The primary effect of such a dopant is, therefore, that doped crystals can be grown at lower temperature gradients than pure crystals. The secondary effect of the dopant is, however, that it interferes with the movement of dislocations in the growing crystal, and thereby decreases the growth speed and changes the growth habit of the crystal.

There are two interesting questions to investigate regarding the possible effects of dopants added during the growth of the crystal:

i. Is the type of incorporation of the dopant the same as with a posteriori doping of an already-grown crystal?

ii. What is the effect of the dopant on the class of the crystal?

During the period of this contract about 80 crystal-growth runs were made, equally divided between "pure" runs and "doped" runs. The pure and doped runs were made under identical growth conditions, so that comparison of the results was possible. T_{WO} growth conditions, H_2S concentration and temperature gradient, were changed over ranges of values which guaranteed a

reasonable amount (10 or more) of usable platelets per run. These ranges were--H_2S concentration: 0-5% vol. (in N_2) and temperature gradient: 5-30° C/cm. The results indicated that in the case of doped crystals the temperature at which the crystal grows becomes an important variable. Less platelets are formed at the low-temperature side of the growth region in doped runs than in undoped runs. It is assumed that this effect is connected with the obstruction of the movement of dislocations by the dopant atoms. At higher temperatures this effect will become less pronounced because of the greater number and mobility of the dislocations. More explicit data will be obtained, in order that we will be able to determine the quantitative influence of this effect on the yield per run.

For detailed investigations of the electrical characteristics of heterojunctions, experimental knowledge about the carrier concentrations and electric field in the junction would be highly useful. In suitably-doped CdS with a blocking contact, information on the electron concentration at the metal-semiconductor boundary and the electric field in the bulk, for zero space charge, can be obtained[13,21]. (See also Sec. 2.a.) The electric-field distribution near the junction in the CdS-region of a Cu_xS-CdS heterojunction is similar to that near a blocking contact. Therefore, in the case of a heterojunction, we expect to be able to obtain information similar to that obtained with a blocking contact. This information is derived through a study of stationary high-field domains (HFD), which are observed under suitable doping conditions in crystals having a range of negative differential conductivity at high electric fields. The quality of the HFD is very sensitive to doping, and to improve reproducibility we carried out a study of the doping procedure. Modifications in the temperature profile of the furnace used during the doping

led to very satisfactory results, which will be detailed below.

Before we discuss the doping per se, we will describe a crystal property which is used extensively in discussions of HFD; namely, $n_1(F)$, the curve of electron concentration vs. electric field for zero space-charge density[21]. In the CdS crystals used this curve is essentially constant up to a "critical" field value. Above this value, n_1 decreases rapidly due to field quenching of the conduction electrons[22]. The critical field at which field quenching sets in and the slope $d(\ln n_1)/d(\ln F)$ in the field-quenching region are key criteria for comparing results in different crystals. The steeper the slope, the better the quality of the domains, as is made evident by experimental observation and explained by the field of directions analysis[13].

Now we will discuss the doping procedure and our results. CdS crystals were doped with differing amounts of silver and compensated with aluminum to produce the necessary negative differential conductivity for the production of HFD. The doping procedure consists of embedding suitable crystals in CdS powder doped with silver and aluminum nitrates and heating to 900° C in an H_2S-N_2 atmosphere for 3 hours. The nitrates dissociate below 500° C and the silver and aluminum are carried into the crystal by diffusion.

The crystals for doping were selected on the basis of high optical quality. Extreme care was taken in the process to prevent the CdS crystals from sintering in contact with the CdS powder at the doping temperatures to preserve the optical quality.

Doped crystals had ohmic Ti/Al electrodes[23] evaporated on them and were tested at 210° K for HFD. The crystals showing good domains were investigated to determine the n_1-curve.

The results of seven doping runs (21 crystals) are very consistent. There appears to be a correlation between doping concentrations and the quality of the stationary domains, in qualitative agreement with the theory[22]. In the case where no aluminum compensation was used, no domains were visible and no current saturation occurred (6 crystals). In the case of 100 ppm Ag, compensated 1:1 with aluminum, domains were observed in every case except one (8 out of 9 crystals). $n_1(F)$ data indicated that the field quenching was not very efficient (i.e., the slope was too shallow). (See Fig. 1.) In crystals doped with 50 ppm Ag and compensated 1:1 with aluminum, all the crystals showed domains (6 out of 6 crystals). The domains had higher field strengths, and field quenching was more rapid and set in at a higher field strength than in those crystals doped with 100 ppm Ag. (See Fig. 1)

Observation of the HFD indicated that the doping was sufficiently homogeneous so as to produce domains of good quality. Also, the $n_1(F)$ curves were highly reproducible at each doping concentration. Thus the doping procedure appears to be sufficiently reliable as to permit us to begin to investigate various properties of the field-quenching mechanism as revealed by the $n_1(F)$ curves. Further investigations will be on the effects of varying the reaction-kinetic parameters in the field- quenching model (i.e., light intensity, infra-red quenching, temperature dependence, etc.). Preliminary work on the variation of light intensity and temperature effects on high field domains in CdS has been started.

In addition to the work described above, we have attempted to measure the parameters influencing the photovoltaic effect in Cu_2S:CdS heterojunctions. The Cu_2S:CdS heterojunction has been made by a chemiplating procedure on CdS single-crystals specially prepared as follows: In order to obtain CdS crystals

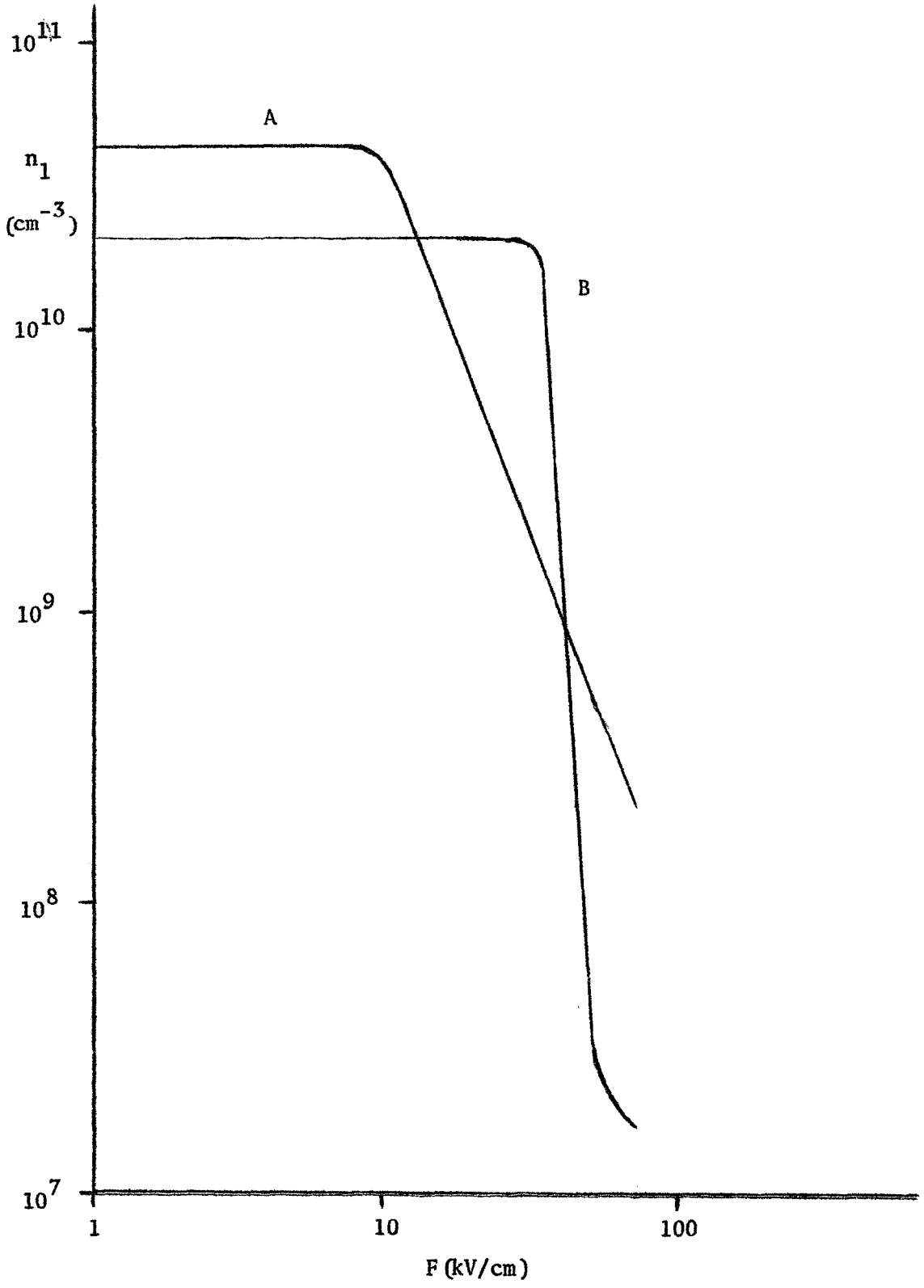

FIGURE 1. $n_1(F)$ curves for two crystals. Crystal A is doped with 100 ppm Ag compensated 1:1 with Al. Crystal B is doped with 50 ppm Ag compensated 1:1 with Al. Results are consistent with other crystals.

with uniform properties, many small crystals were cut from a single platelet at Jet Propulsion Laboratory (Dr. Stirn). Since the dimensions of these crystals were approximately 300 x 200 x 80 microns, special techniques were developed to handle them: One of these crystals was placed on a glass slide and encapsulated in an epoxy (Sylgard 51 Dielectric Gel made by the Dow Corning Company) which was cured at 75° C for 3/4 to 2 hours. A face of the crystal perpendicular to the c-axis was exposed by cutting away the epoxy with a razor blade. Then a Ti/Al contact (supposedly ohmic) was evaporated onto the exposed face.

The crystal was then potted in the epoxy again which was cured as before. This time the opposite face of the crystal was exposed and dipped in a 25% solution of HCl for about a minute. After this the crystal was dipped in a saturated aqueous solution of CuCl kept at 90° C for 1/2 to 1-1/2 hours. This formed a Cu_2S layer 20 to 50 microns thick on the CdS crystal.

The CuCl solution was prepared by first dissolving $CuCl_2$ in concentrated HCl and Cu. This was boiled until the liquid turned clear. Then cold H_2O was added to precipitate out the CuCl. The CuCl was washed three or four times with water before heating.

With the junction on, the crystal was removed and placed on another glass slide. Here contact was made to the Cu_2S and Ti/Al by Cu wires cemented to the crystal with silver print.

Because of mechanical difficulties (caused by the smallness of the crystal) in making a uniform junction and making contact to this junction, only one crystal has gone through this procedure successfully enough to make electrical measurements. The Ti/Al contact on this crystal was not ohmic, so measurements were made only at high voltages. With the Cu_2S layer used

as the cathode, a cathode-adjacent high-field domain appeared along with current saturation. The field strength in this domain was approximately 60 k V/cm at a temperature of 200° K.

A larger-sized CdS crystal has been prepared with a Ti/Al ohmic contact and a Cu_2S heterojunction. The current-voltage characteristics of this device have shown highly-rectifying behavior and an open-circuit voltage somewhat greater than .25 volts under illumination at room temperature. This compares favorably with other reports[24]. These measurements will be compared with those from the smaller crystals.

Now that the methods of preparing the junctions on the CdS crystals have been established, the measurement of the electrical parameters of the devices should proceed rapidly.

(c). In order to produce photovoltaic cells which operate reliably under actual working conditions, information must be obtained concerning the effects of radiation damage and the ambient atmosphere on the photoelectric parameters of the cells. Investigations of these effects, to be discussed below, show that CdS single crystals fall into two classes. The existence of these two classes was first pointed out in another connection by E. F. Gross and B. V. Novikov[20]. They defined Class I crystals as those for which the spectral dependence of photoconductivity (SDP) at liquid-nitrogen temperature (LNT) showed maxima which coincided with maxima in the free-exciton absorption spectrum and Class II crystals as those for which minima in the SDP coincided with maxima in the absorption. This separation of CdS crystals into two classes was found to hold with respect to various properties[25,26]. Some of the previous work already contained the idea that the differences in behavior

of the two classes arose because of differences in surface and bulk photoconduction properties.

The relevant results we obtained on the two classes of crystal will be discussed below. The first consideration in an experiment, of course, is to decide which class the crystal we are making measurements on belongs to. This is accomplished by making use of the following characteristics of Class I and Class II crystals: Class I CdS crystals exhibit a strong green-edge photoluminescence and a shoulder in the SDP at room temperature, while Class II crystals show no green-edge photoluminescence and exhibit a peak in the room-temperature SDP[2,27]. Also, the two classes show different thermally-stimulated desorption curves (TSD) for oxygen (AMU 16)[1,2].

Now we will discuss the first set of measurements[1,2]. They were initiated in order to help us to understand the electrical and optical properties of Class I crystals[1,2,27]. It is observed that an increase of several orders of magnitude of the SDP results if a Class I crystal is heated in ultra-high vacuum (10^{-9} torr) to a temperature of 275° C. Further heating of the crystal causes the SDP to decrease until a temperature of 400° C has been reached. At this temperature the Class I crystal becomes a Class II crystal. The SDP of the Class I crystal is reversible upon oxygen backfill as long as the crystal has not been heated to a temperature in excess of 275° C (Fig. 2).

Mass spectroscopic measurements[1] in ultra-high vacuum of the thermally desorbed gases from Class I crystals show that oxygen (AMU 16) is desorbed from the crystal, starting at a temperature of 135° C and reaching a maximum at 325° C. The activation energy for desorption is 0.75 eV and the surface concentration is ~ 10^{15} atoms $-cm^{-2}$ (Fig. 3). Similar measurements of thermally-desorbed cadmium show that cadmium desorption starts at 275° C, goes

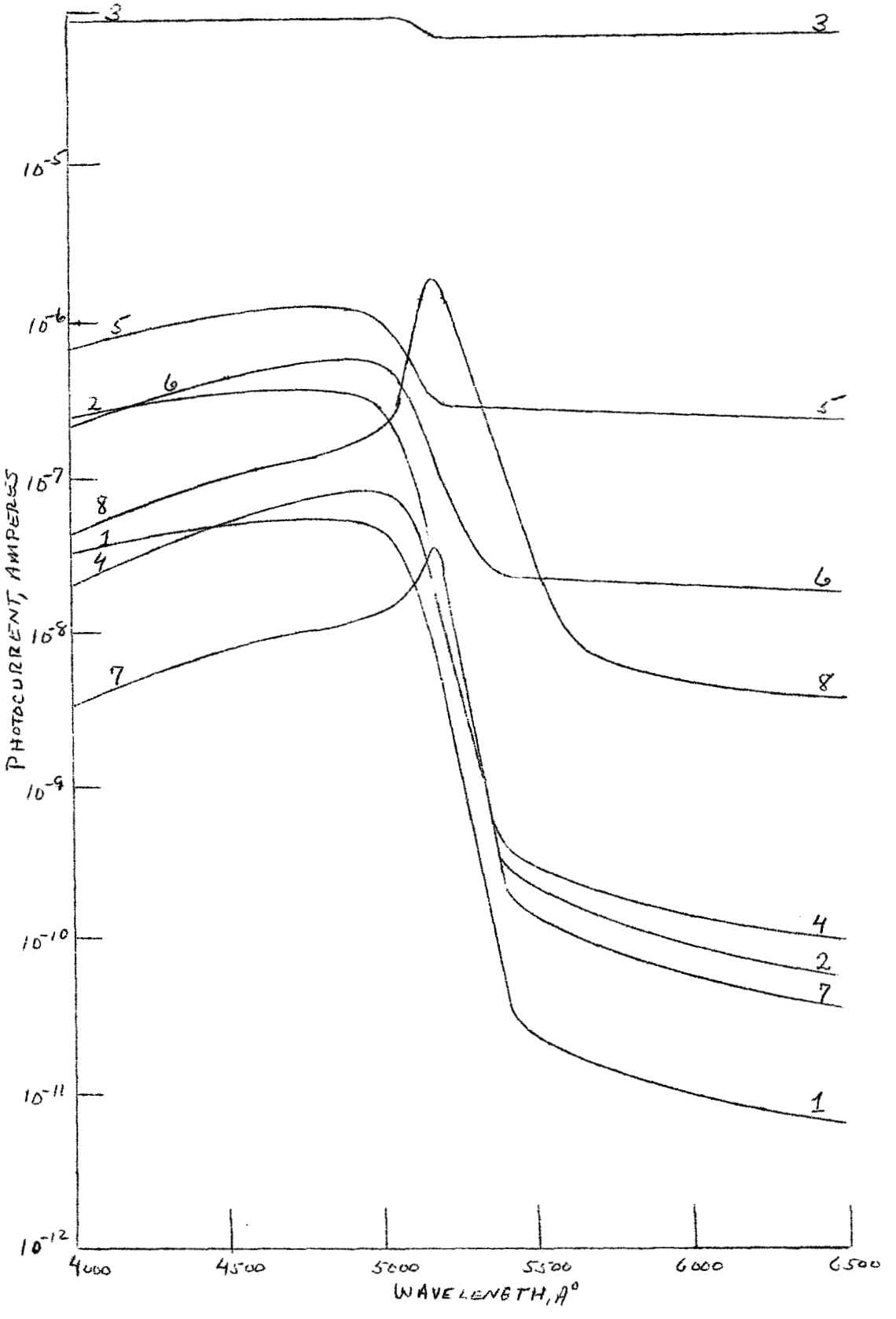
PHOTOCURRENT, AMPERES
10^{-5}
10^{-6}
10^{-7}
10^{-8}
10^{-9}
10^{-10}
10^{-11}
10^{-12}
4000
4500
5000
5500
6000
6500
WAVELENGTH, A°
3
5
6
2
8
1
4
7

FIGURE 2

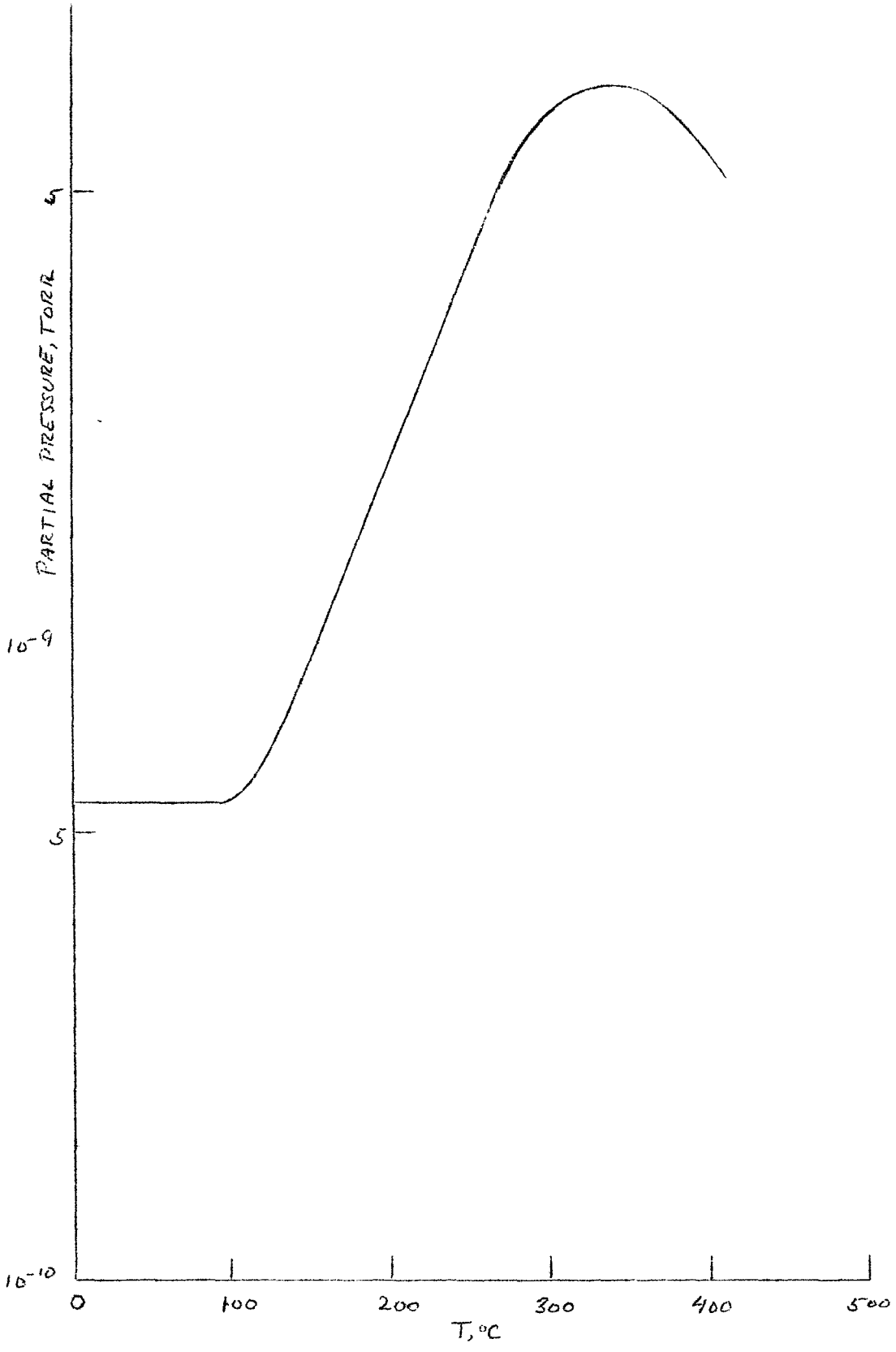

FIGURE 3

Figure Captions

FIGURE 2. Spectral Dependence of Photoconductivity measurements showing the transition of a Class I crystal to a Class II crystal, -- all measurements taken at room temperature.

1 Pressure of 1 atm air - Virgin Class I crystal
2 $P = 10^{-9}$ torr
3 $P = 10^{-9}$ torr - after heating to 275° C
4 P = 1 atm O_2
5 $P = 10^{-9}$ torr - after heating to 365° C
6 $P = 10^{-9}$ torr - after heating to 380° C
7 $P = 10^{-9}$ torr - after heating to 400° C
8 $P = 10^{-9}$ torr - after heating to 525° C

FIGURE 3. Thermal Desorption Spectrum of oxygen from a Class I crystal.

through a plateau at 450° C, and starts a very abrupt increase at 500° C. The initial activation energy for desorption is 1.32 eV and the associated surface concentration is ~ 10^{13} atoms -cm^{-2} (Fig. 4).

The temperature of the crystal is determined by monitoring the thermally-induced shift of the band edge[28], and the heating is accomplished by the Joule's heating of the crystal itself under an applied voltage of 800 V. DC which is controlled by a feedback circuit monitoring the band-edge shift. Typical heating rates are 8-10° K/sec. In all cases the SDP measurements are taken after the crystal has returned to room temperature.

It has been observed[1] that when a Class I crystal has been converted to a Class II crystal, the Class I state can be partially restored by a 3.5 keV electron bombardment for two hours with a beam current density of ~ 10^{-7} amps -cm^{-2}. This restoration is accomplished by the 'knocking-out' of the surface near sulfur atoms thus producing an excess cadmium layer in the surface-near region. This restored surface layer of cadmium is seen in subsequent mass spectroscopic measurements of thermally induced desorption. (Fig. 5).

For the second set of measurements, namely, luminescence and SDP at liquid N temperature, selected CdS platelets of Class I with evaporated Ti/Al electrodes (slit geometry with 5 x 5 mm^2 uncovered CdS and about 100 μ width) were mounted in a thermally-shielded crystal holder within a vacuum chamber. The platelets used were grown in our laboratory by the sublimation of CdS powder, cooled at 2° C/min. in an N_2-H_2S (1%) atmosphere. In this case, as opposed to the first set of measurements, the crystal was heated up by means of a heater attached to the Cu crystal holder and its temperature determined with a thermocouple.

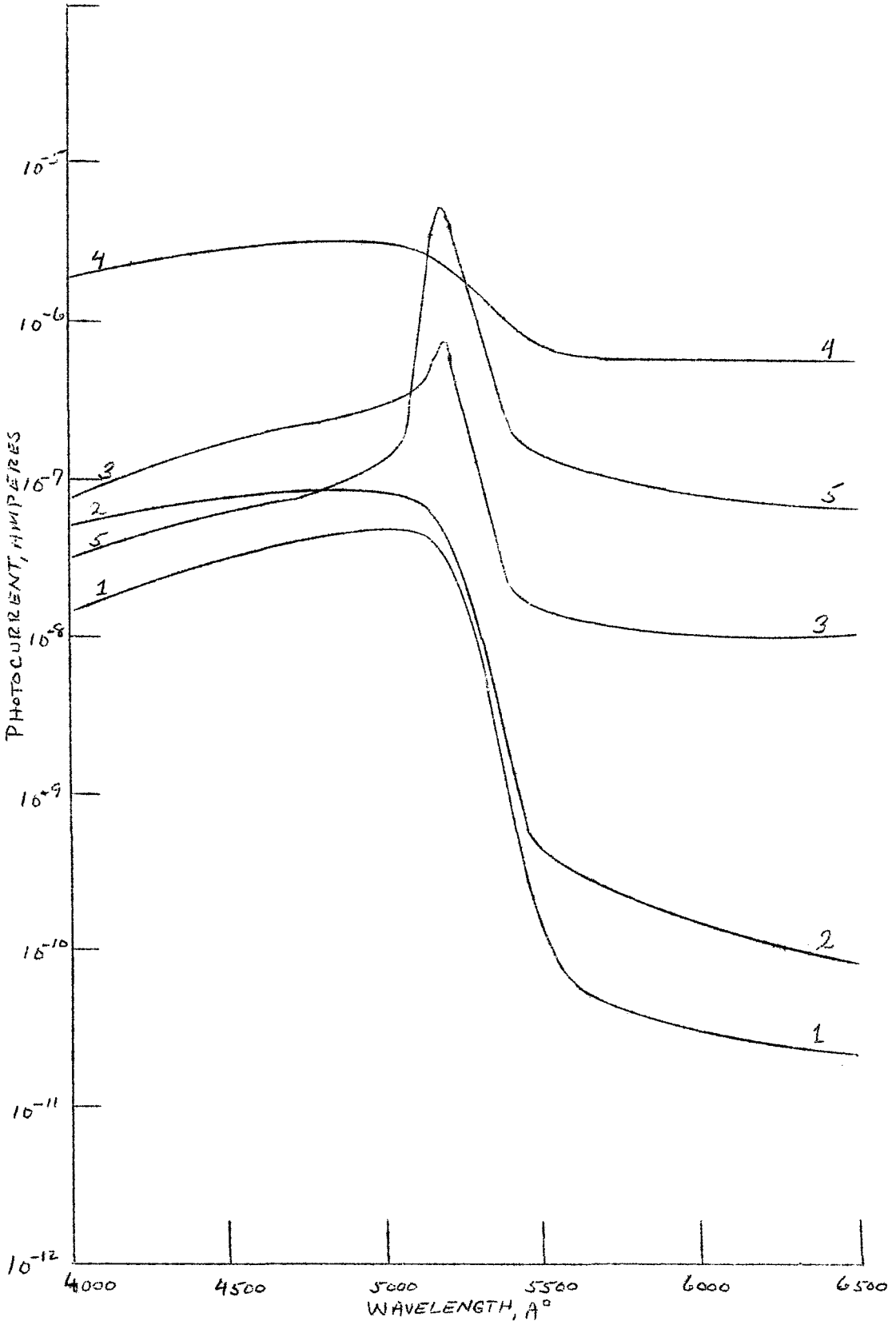
PHOTOCURRENT, AMPERES
10^{-5}
10^{-6}
10^{-7}
10^{-8}
10^{-9}
10^{-10}
10^{-11}
10^{-12}
4
3
2
5
1
4
5
3
2
1
4000
4500
5000
5500
6000
6500
WAVELENGTH, A°

FIGURE 4

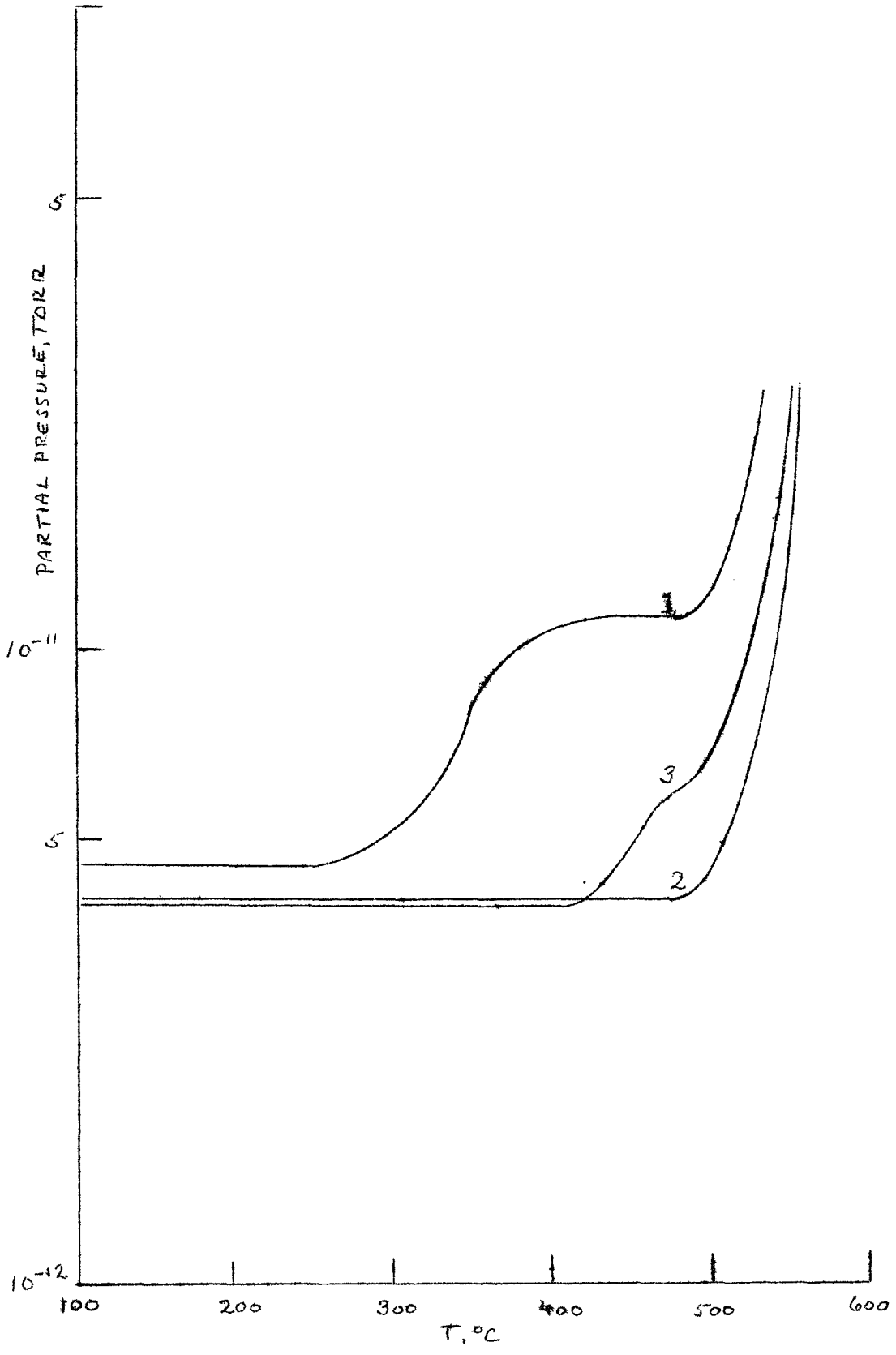

FIGURE 5

Figure Captions

FIGURE 4. Spectral Dependence of Photoconductivity measurements showing the transition of a Class I crystal to a Class II crystal and the subsequent restoration of the crystal to the Class I state by electron bombardment.

1 Pressure of 1 atm air - Virgin Class I crystal
2 $P = 10^{-8}$ torr
3 $P = 10^{-8}$ torr - after heating to 550° C
4 $P = 10^{-8}$ torr - after 3.5 keV electron bombardment for two hours
5 $P = 10^{-8}$ torr - after heating to 550° C

FIGURE 5. Thermal Desorption Spectrum of cadmium from a Class I crystal

1 Initial desorption of Virgin crystal
2 Subsequent desorption immediately following 1
3 Desorption after 3.5 keV electron bombardment

The spectroscopic analysis was done with a 1m-Jarrell-Ash spectrometer used as a monochromator for luminescence (1.2 Å spectral slit width) and photoconduction (3 Å spectral slit width) measurements. For luminescence excitation an HBO-200-Mercury lamp with a 365 nm and a heat glass filter was used.

The luminescence was measured at LNT before and after heat treatments. The luminescence spectrum of the virgin crystal showed the characteristic green-edge emission, with a central peak at about 5150 Å and its phonon replicas, separated by .038 eV (about 80 Å), and also a peak at about 5400 Å. Most sensitive to a heat treatment in vacuum was the green-edge emission, which showed for all investigated crystals a marked decrease between 150 and 200° C. This emission always disappeared below detection limits after treatment near 250° C.

The SDP at LNT, when scanned from shorter to longer wavelengths after pre-illumination at about 4840 Å, showed excellent reproducibility and the typical Class I behavior. After heat-treatment at 200° C the shape of the curves changed completely to become characteristic of Class II crystals.

The room-temperature SDP was also measured before and after heat-treatments and also indicated a change from Class I to Class II features. In agreement with previous results, a marked increase in the dark current was observed. The difference between the temperatures for which the transition from Class I to Class II occurs, as determined from the experiments above with different heating methods, can be attributed to the fact that in the second case, with a lower heating rate, the crystal spends more time at the higher temperatures.

It is possible to explain the above results if one assumes that the electrical and optical properties of a Class I crystal are determined by a thin (~ 10^{-5} cm) surface-near layer containing excess Cd compensated by adsorbed 0. Desorption of this 0 causes the photoconductance to increase (by electronic sensitization) without altering the class of the crystal. Diffusion of Cd into the bulk and Cd evaporation take place during heat-treatment between 300 to 400° C, thereby increasing the relative contribution of the bulk to the photoconduction process. Thus, the crystal becomes a Class II crystal. The restoration of the Class I behavior of the crystal upon electron bombardment at 3.5 keV is attributed to a re-enrichment of the surface-near region with Cd. (See ref. 2 for further details.)

The difference between the LNT SDP in the exciton region for Class I and II CdS crystals arises from the difference in photosensitivity (lifetime) across the width of the crystal[29].

Investigations into the reasons for the changes in luminescence from Class I to Class II are continuing. It is interesting to note that luminescence may be influenced by a space-charge region caused by gases adsorbed on the surface of CdS, since in this region carriers are redistributed over levels in the band gap. Therefore, helpful information for the identification of luminescent transitions and of excitons bound to defect centers can be obtained from these studies.

The preceding considerations demonstrate the importance of further research into the surface characteristics of CdS. Of particular interest is the measurement of all properties involved in the previous research, simultaneously on one crystal. Current work underway in our laboratories is concerned with these measurements as carried out on both halves of a cleaved CdS single-crystal of Class I.

The changes in the luminescence spectrum and SDP at LNT, the SDP at room temperature, and the thermally-stimulated current curves (TSC) for intrinsic and extrinsic excitation are being studied as a function of treatment temperature on one of the two halves. Details are discussed below. For the other, its electrical properties as well as TSD curves have already been determined, the results being typical of a Class I crystal going to Class II upon heat treatment. The crystal used in these experiments was grown in our laboratories under the same conditions of the crystals used in previous experiments (see sec. 2.b.). It has the same geometry and size (5 x 5 x 0.1 mm^3). Ti/Al contacts were evaporated onto the whole crystal before cleaving. Pt leads were shown to yield more reproducible results than either Au or Al.

The following results were obtained with the crystal in the virgin state: The SDP at room temperature was determined before and after pumping the crystal atmosphere down to 10^{-9} torr. The results are typical of a Class I crystal, as are the changes that occurred upon pumping: A general displacement of the SDP towards higher currents and an increase in the dark current took place[2].

At LNT and after pumping, the SDP showed the expected (for a Class I crystal) coincidence between exciton peaks in the photoconductance and the absorption[27].

Finally, the luminescence (photoemission) spectrum at LNT exhibited a strong green-edge luminescence series, plus two weaker peaks at 4900 Å and 5460 Å (approximately).

For the virgin state, the TSC with intrinsic and extrinsic preillumination, and the dark current as a function of temperature between LNT and room temperature were also determined.

When the crystal was heat-treated, the results obtained were as follows: No major changes in any of the previously determined properties were observed upon treatments up to 100° C.

The electrical properties of the crystal were observed to be strongly affected by the ultra-violet excitation used during emission measurements. However, they essentially reverted to their previous behavior after a period of about ten days, with the exception of a slight remaining shift towards higher values in the SDP and the dark current. This remaining shift was always eliminated after a TSC run to 100° C.

The SDP at room temperature was found to depend also on pre-illumination, unless the crystal was allowed to sit in the dark for about 4 or 5 days. However, a period of only one day in the dark insures good reproducibility while saving time. This investigation is being continued with heat-treatments at higher temperatures.

The final set of measurements concerns radiation damage. It is possible to discuss radiation damage of CdS within a general scheme once the classification of CdS crystals has been clarified. It is necessary to consider the two classes separately since the region of the crystal (i.e., the near surface layer or the bulk) involved in photoelectronic properties is quite different for the two crystal classes.

In previous measurements by O'Connell[30] a threshold for damage was found to be approximately 300 keV in a vacuum of 10^{-9} torr. Class II crystals were tested. A decrease in electron lifetime was observed. In more recent experiments[31] on Class II crystals, it was found that the damage threshold was less than 250 keV for an ambient pressure of ~ 10^{-8} torr. Since the SDP curve made a parallel shift upward as a result of the radiation, it is believed that a decrease in recombination center density occurred although an

increase in hole traps is a possibility, thereby resulting in a longer electron lifetime. The TSC curves for Class II crystals showed an increase in levels around 300° K in agreement with O'Connell. These levels were attributed to an increase in sulfur vacancies by him. (It should be noted that a general increase in the TSC occurred over the temperature range. However, the change at 300° K was more than a parallel shift.)

The result for the damage threshold is considerably higher than that found by Kulp and Kelley[32]. There are two possible reasons for this. One, the X-rays that were used were distributed in energy and not monochromatic. Relatively few photons had an energy near the maximum accelerating potential of the X-ray machine -- that is, the largest number of photons had energies significantly less than the maximum. As a consequence, the dose received by the crystal at a given energy becomes important. Secondly, it is possible that the ambient pressure in the vacuum chamber had a significant effect on the threshold. Residual gases might be ionized and impact the surface of the crystal thereby causing structural changes. A much lower ambient pressure would eliminate this possibility. Kulp and Kelley irradiated their samples with electrons in a vacuum of 10^{-5} torr whereas O'Connell used X-rays in a 10^{-9} torr vacuum. In the more recent experiments[31] vacuums from 10^{-7} torr to 10^{-8} torr were used in Class II crystals.

The situation with Class I crystals appears to be quite different from Class II crystals regarding the damage threshold. The recent experiments[31] indicate that the damage threshold is below 200 keV. Considerable upward shifts were noticeable in both the intrinsic and extrinsic range although the peak current did not change too much. The shift in the extrinsic region was greater than that in the intrinsic region. Also, a sensitivity to 6000 -

6500 Å illumination appeared that was previously lacking. TSC curves indicated an overall increase of electrons in traps; no defined trapping level appeared as a result of irradiation. It is not immediately apparent as to what is responsible for the observed changes since the near-surface layer is important in this class of crystal. However, it is apparent that the lifetime of electrons was increased.

Because the near-surface layer is particularly important in Class I crystals, any change in the surface layer might be particularly apparent. For example, residual gas in the vacuum chamber that might be ionized by the incident radiation could cause substantial changes in the photo-electronic properties of the crystal. Kulp and Kelley[32] reported that the green edge luminescence could be made to disappear by bombarding crystals with electrons having energies ranging from 3 keV to 200 keV. As stated previously, their pressure was 10^{-5} torr during irradiation. It is conceivable that the use of X-rays and much lower ambient pressures might result in higher energies being necessary to cause damage to the crystal. Therefore, further studies of Class I crystals are necessary to find out the damage threshold, the effect of ambient pressure and heat treatment, and the defects that are responsible for the substantial changes observed.

At the present time, the pre-irradiation characterization of a Class I crystal has been done. Figure 6 shows the room-temperature and LNT SDP. Figure 7 shows the thermally-stimulated current curve. The room-temperature SDP shows the characteristic shoulder around 4800 Å with a subsequent three orders-of-magnitude drop in the photocurrent by 6500 Å. The LNT SDP shows almost 5 orders-of-magnitude difference between the intrinsic and extrinsic regions. The thermally-stimulated current curve shows the presence of electronic traps at approximately 195° K and 250° K.

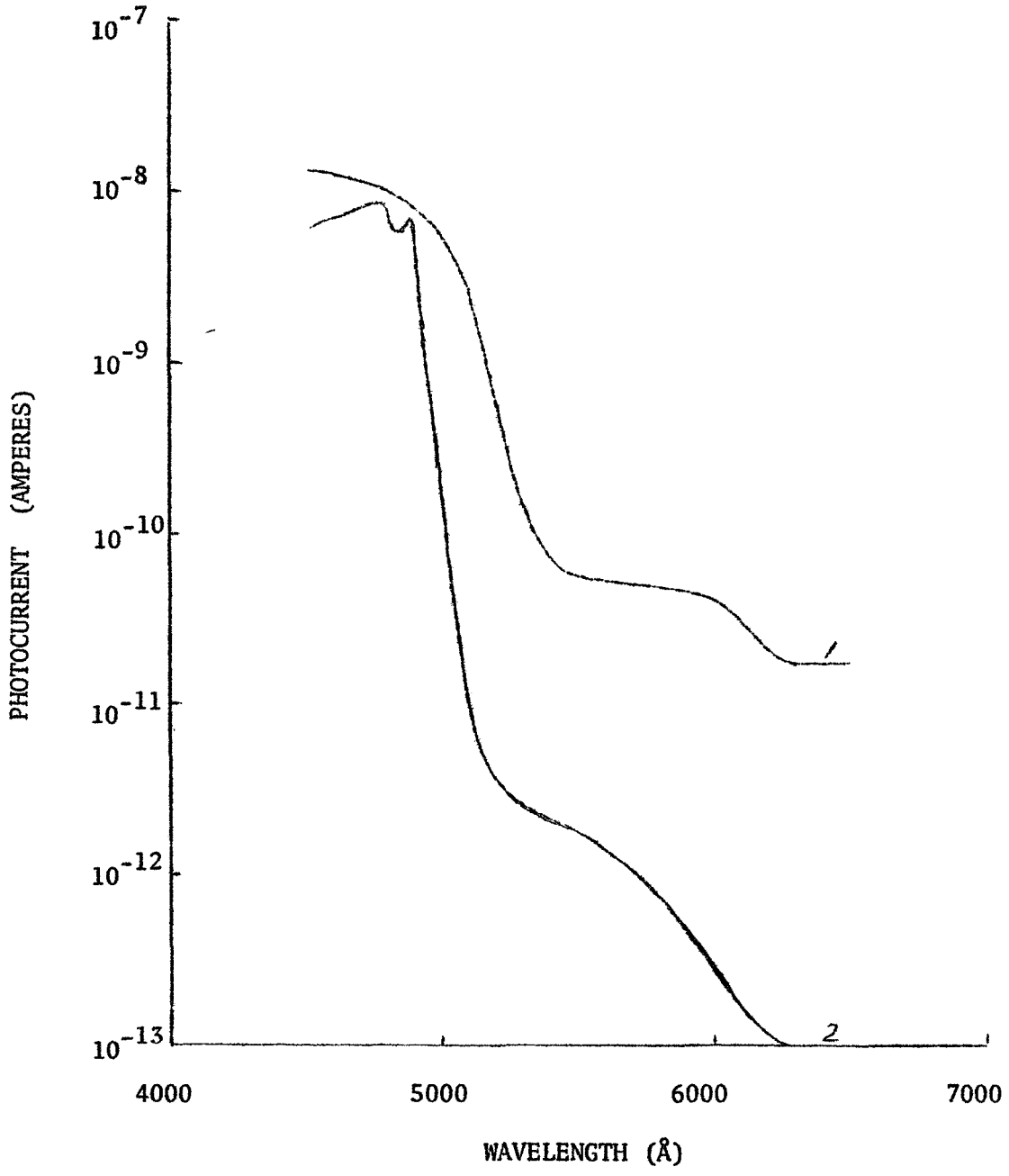

FIGURE 6. Pre-irradiation spectral dependence of photoconductivity curves for a Class I CdS crystal. Curve 1: room temperature; curve 2: LN_2 temperature.

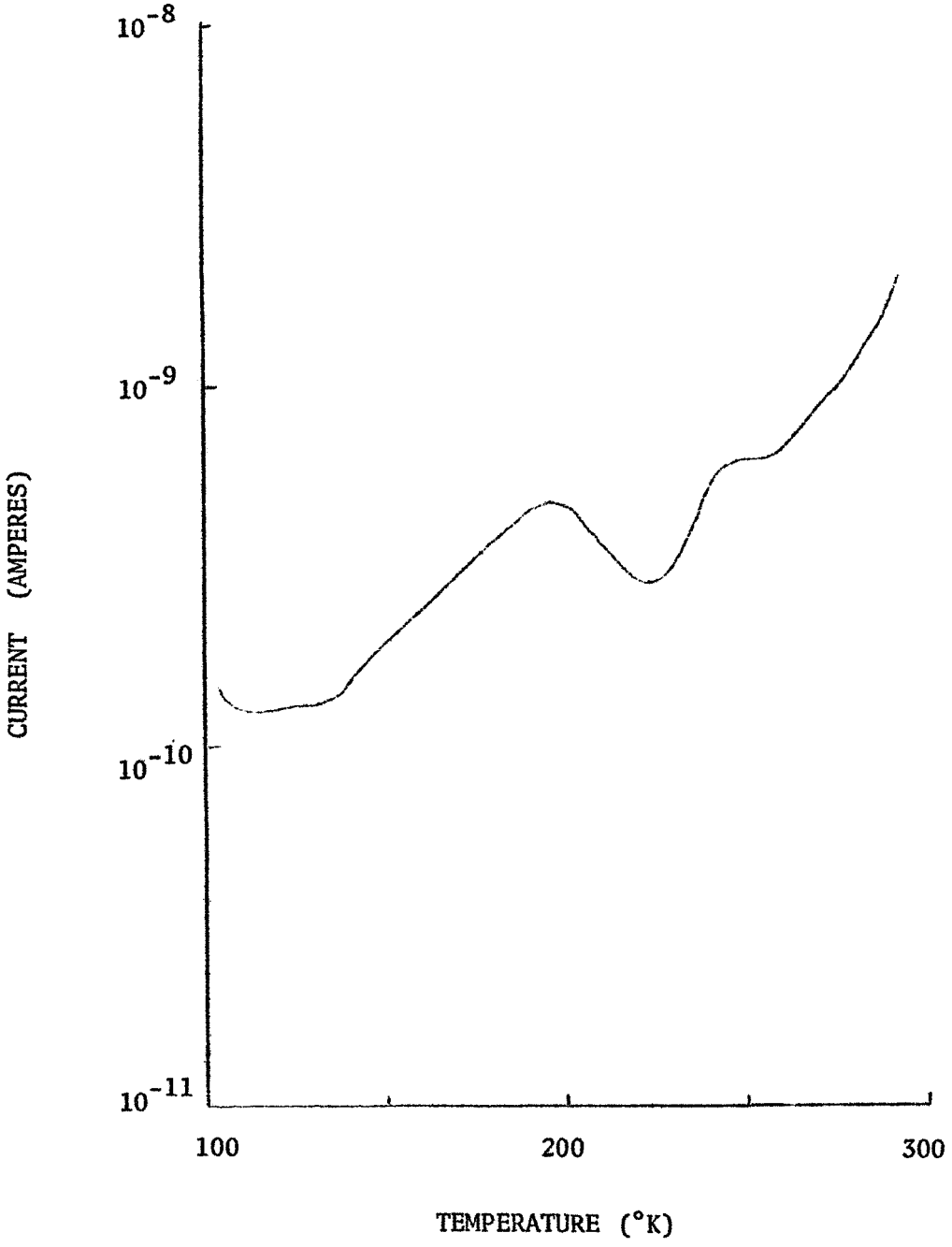

FIGURE 7. Pre-irradiation thermally stimulated current curve for a Class I CdS crystal.

As the irradiation of a Class I crystal has not yet been done, the following is a proposed procedure. After obtaining a pressure of 10^{-8} torr or less, measurements of the spectral dependence of the photoconductivity at room and LNT and the thermally-stimulated currents are made in order to characterize the pre-irradiation state of the crystal. Then, the following outline indicates the path of investigation.

We take a virgin crystal and irradiate it with 150 keV radiation at 10^{-8} torr.

1. If there is damage, we subject the crystal to temperature treatments starting at 50° C and increasing by 50° C at each treatment. After each treatment the crystal is subjected to 150 keV irradiation at 10^{-8} torr.
2. If there is no damage, we irradiate the crystal with 150 keV radiation at 10^{-5} torr. If there is no damage, of course, we don't anneal. In either case, we then subject the crystal to 200 keV irradiation at 10^{-8} torr.
    a. If there is damage, we subject the crystal to temperature treatments starting at 50° C and increasing by steps of 50° C. After each treatment we irradiate the crystal at 200 keV and 10^{-8} torr.
    b. If there is no damage we irradiate the crystal with 200 keV at 10^{-5} torr. If there is damage, we anneal the crystal. If there is no damage, we don't anneal. Then in both cases we irradiate with 250 keV at 10^{-8} torr.

The above pattern is continued.

By this procedure, the threshold energy for damage, the effect of of ambient pressure, and the effect of temperature are to be determined.

3. CONCLUSIONS

In the first phase (1/6) of the proposed research effort to improve the quality of CdS photovoltaic cells, specifically to improve the conversion efficiency over the currently achieved ~ 5%, the following results and conclusions were arrived at:

1. A research team of nine scientists/students (mostly working part-time for this contract) was formed (total effort will average about 3 man/year), and this team was familiarized with the general state of the art and the goal in photovoltaic research.

2. Three research groups within this team were established with close coordination of their research in the fields of (a) photovoltaic theory, (b) material, and (c) influence of external means (radiation, ambient atmosphere).

3. The results of the theoretical group with respect to the junction analysis are encouraging. The consistent discussion of the Poisson- and extended transport equation[12] using a graphical approach yields very useful results and shall be continued.

4. The discussion of the kinetics of the field distribution near a contact is very helpful because of two reasons:

   (a) At least one contact of a photovoltaic cell will be close to the active volume of the cell for maximum efficiency.

   (b) The field distribution in a heterojunction is very similar to the one near a contact and most of the results obtained can readily be used for the junction.

We have used this approach since here experimental results were already available. The theory shall be expanded for junctions.

5. The use of high-field domains for obtaining further experimental information on the field distribution and electron concentration within the junction shall be further analysed after such domains have been observed experimentally.

6. The experimental group involved in crystal growth, doping and production of the heterojunction has successfully completed this task with respect to CdS-platelet/Cu_xS junctions with CdS-doping as required for high-field domains. For the second phase of this program the single-crystal approach shall be continued since here an analysis of the photovoltaic parameters can be performed in a more transparent way than for evaporated or sintered layers.

7. Attention shall now be focussed on systematic changes in CdS and junction parameters (as, e.g., CdS doping and junction gradient with graded composition).

8. Preparations shall be made to start using simultaneously epitaxially grown, evaporated and recrystallized, or sintered CdS layers beginning in the third phase of the program (Fall 1970).

9. The investigation on the influence of the ambient atmosphere on photoelectric parameters was successfully concluded with respect to oxygen. This part resulted in a short note (already published[1]) and a paper (submitted for publication[2]). A few more experiments will be made to obtain additional quantitative results necessary for proper doping and surface deactivation.

10. These experiments shall be extended to analyse and minimize the influence of water vapor.

11. X-ray damage experiments have shown a first threshold of some CdS platelets in 10^{-5} torr air ambient at 115 keV, -- other platelets in 10^{-9} torr ambient have the first threshold at ~ 275 keV. Doping differences and ambient atmosphere may be reasons for this difference in threshold. Also some differences in annealing temperatures are detected. Such findings can become important for producing highly damage-resistant photocells and intensive further research is planned in this area.

4. RECOMMENDATIONS

Since the research program was started only six months ago, most of the findings are of preliminary nature and recommendations are made with reservations. The results have to be solidified so that we can make sound and detailed suggestions for improvement.

With some candor therefore the following suggestions are made:

1. For maximum open-circuit voltage the material should be doped in such a way that the (dark) Fermi-level lies close to the respective band and the quasi-Fermi-level for minority carriers shifts as close as possible to the opposite band with light. A small density of levels in the center part of the band gap seems essential for this.

2. Material which is more than a random-walk length for minority carriers separated from the junction is useless for the photovoltaic effect and can only reduce it because of additional optical absorption. It should also be eliminated because it acts as undesired series resistance which can only be neglected for high doping levels, which in turn are undesired since they oppose point 1 of these recommendations.

3. Since the random-walk length of minority carriers and the Debye screening length are of the order of (or below) 10^{-5} cm, only a very thin

slab of the (not graded) photovoltaic device is active; hence large optical absorption ($\kappa \gtrsim 10^5$ cm^{-1}) is required for efficient photogeneration of carriers. This requires extreme doping densities in the junction, i.e., grading of the junction and illumination through the wide band gap material for maximum efficiency. The thickness of the graded part should not exceed the Schubweg of the minority carriers in the junction field.

4. For efficient transport of the carriers to the electrodes the width of each side of the device (measured from the centerplane of the junction) shall be smaller than the random-walk length of the majority carrier.

This asks for rather thin backwall devices (less than 1 μm). Technical difficulties in producing thin pinhole-free layers with perfectly laminated graded junction determine the currently used optimum thickness of about 100 x the theoretical optimum. Therefore intensive studies of economical means of laminated deposition of thin graded junctions are highly recommended. The development of a highly transparent front-electrode (e.g., n^+-CdS) with an ohmic metal grid (Ti/Al) is suggested.

5. NEW TECHNOLOGY

In the first phase of this contract no new technology was developed. Investigation pertinent to such development will start in the third phase (Fall 1970).

6. REFERENCES

1. C. Wright and K. W. Böer, Phys. Stat. Sol. 38, K51 (1970).
2. R. Schubert and K. W. Böer, to be published in J. Phys. Chem. Sol.
3. W. Palz and W. Ruppel, Phys. Stat. Sol. 6, K161 (1964).
4. L. R. Shiozawa, G. A. Sullivan and F. Augustine, Proc. of the 7th Photovoltaic Specialists' Conf., Pasadena, Calif. (1968) (unpublished).
5. R. Marshall and S. S. Mitra, J. Appl. Phys. 36, 3882 (1966).
6. N. Nakayama, Jap. J. Appl. Phys. 8, 450 (1969).
7. G. P. Sorokin, Yu. M. Papshev and P. T. Oush, Sov. Phys.-Solid State 7, 1810 (1966).
8. G. B. Abdullaev, Z. A. Aliyarova, E. H. Zamanova and G. A. Asadov, Phys. Stat. Sol. 26, 65 (1968).
9. B. Agusta and R. L. Anderson, J. Appl. Phys. 36, 206 (1965).
10. L. J. van Ruyven and I. Dev, J. Appl. Phys. 37, 3324 (1966).
11. Y. Marfaing, G. Cohen-Solal, and F. Bailly, Physics of Semiconductors, p. 1245, Dunod, Paris (1964).
12. L. J. van Ruyven and F. E. Williams, Am. J. Phys. 35, 705 (1967).
13. K. W. Böer, G. Döhler, G. A. Dussel, P. Voss, Phys. Rev. 169, 700 (1968).
14. K. W. Böer, G. A. Dussel, P. Voss, Phys. Rev. 179, 703 (1969).
15. R. Stirn, K. W. Böer, G. A. Dussel, P. Voss, Proceedings of the International Conf. on Photoconductivity, Stanford (1969) (in print).
16. A. J. Bennett and C. B. Duke, Phys. Rev. 160, 541 (1967); Phys. Rev. 162, 578 (1967).
17. G. H. Parker, C. A. Mead, Appl. Phys. Lett. 14, 21 (1969).
18. G. A. Dussel, K. W. Böer, Phys. Stat. Sol. 39, (1970) (in print), (first paper).

19. W. Franz, Handbuch der Physik, XVII, 153 (1956).
See, e.g., G. A. Dussel, Ph.D. Dissertation, University of Delaware, 1970.

20. E. F. Gross and B. V. Novikov, J. Phys. Chem. Sol. 22, 87 (1961).

21. K. W. Böer and P. Voss, Phys. Rev. 171, 899 (1967).

22. G. A. Dussel and K. W. Böer, Phys. Stat. Sol. 39, (1970) (in print) (second paper).

23. K. W. Böer and R. Hall, J. Appl. Phys. 37, 4739 (1966).

24. L. R. Shiozawa, F. Augustine, G. A. Sullivan, J. M. Smith, III, and W. R. Cook, Jr., Final Report, Contract AF 33 (615)-5224, Aerospace Research Labs, May 1969, pp. 98-99.

25. E. F. Gross, J. Kh. Akopian, F. I. Kreingold, B. V. Novikov, R. A. Titov, and R. I. Shekhmametiev, Proc. of the Seventh Int. Conf. on Semiconductors, Paris (1964) p 957.

26. D. C. Reynolds, C. W. Litton, and T. C. Collins, Phys. Stat. Sol. 9, 645 (1965).

27. J. Bragagnolo and K. W. Böer, J. of Luminescence 1 (in print).

28. H. Radelt, Z. Naturf. 15a, 269 (1960).

29. J. Voigt and E. Ost, Phys. Stat. Sol. 33, 381 (1969).

30. J. O'Connell, Ph.D. Thesis, Univ. of Delaware, 1967.

31. K. W. Böer, Contract Report NAS1-8787, NASA-Langley Research Center, November, 1969.